Supporting Information

Fluorinated Zr-MOF Modified Separators for Li-S Batteries with Enhanced Electrochemical Performances

Yang-Jie Wang[#,a], Lei Cao[#,b], Hai-Xin Li[a], Bao-Qun Wang[b], Jin-Shan Xiong[a], Jun-Jie Zhang[a], Jin-Liang Zhuang*[,a], Xuan Du*[,b], Wei Zhao*[,b]

[a] School of Chemistry and Materials Science,Key Laboratory for Functional Materials Chemistry of Guizhou Province, Guizhou Normal University, Guiyang 550001, PR China

[b] Institute of ProcessEngineering, Chinese Academy of Sciences, Beijing 100190, China PR China. E-mail: wzhao@ipe.ac.cn

# These authors contributed equally to this work.

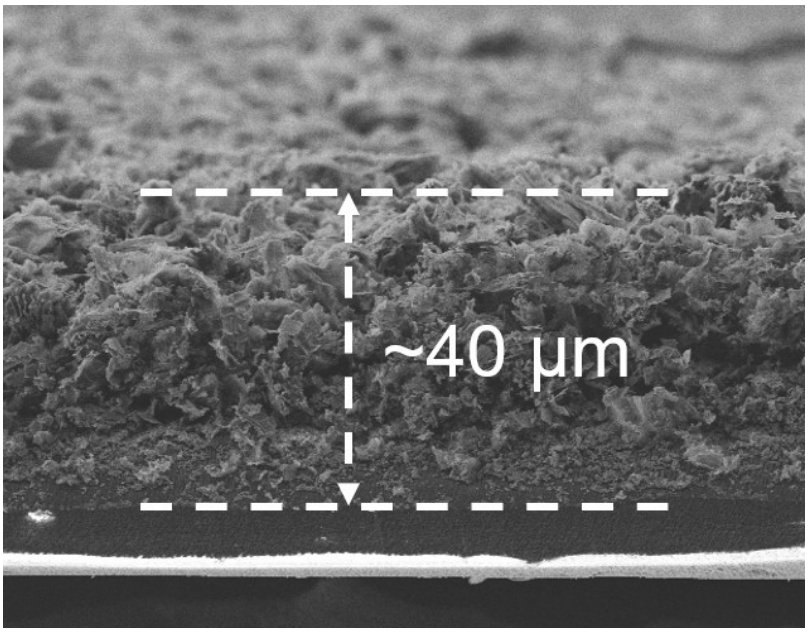

Fig. S1 SEM image of UiO-66-4F modified separator cross-section.

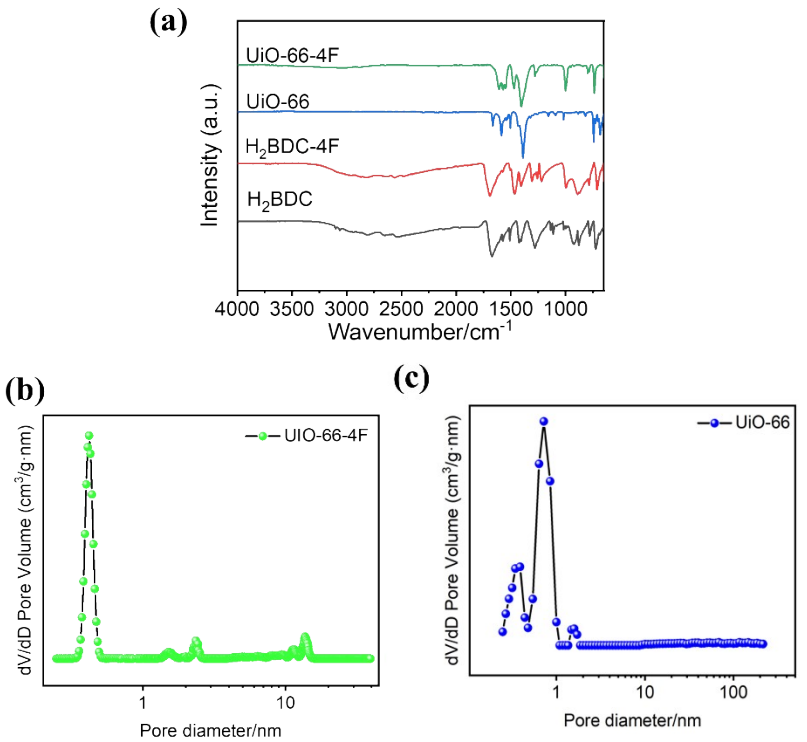

Fig. S2 (a) FTIR spectra of UiO-66-4F, UiO-66, and their corresponding ligands. (b-c) DFT calculated pore size distribution of UiO-66-4F and UiO-66.

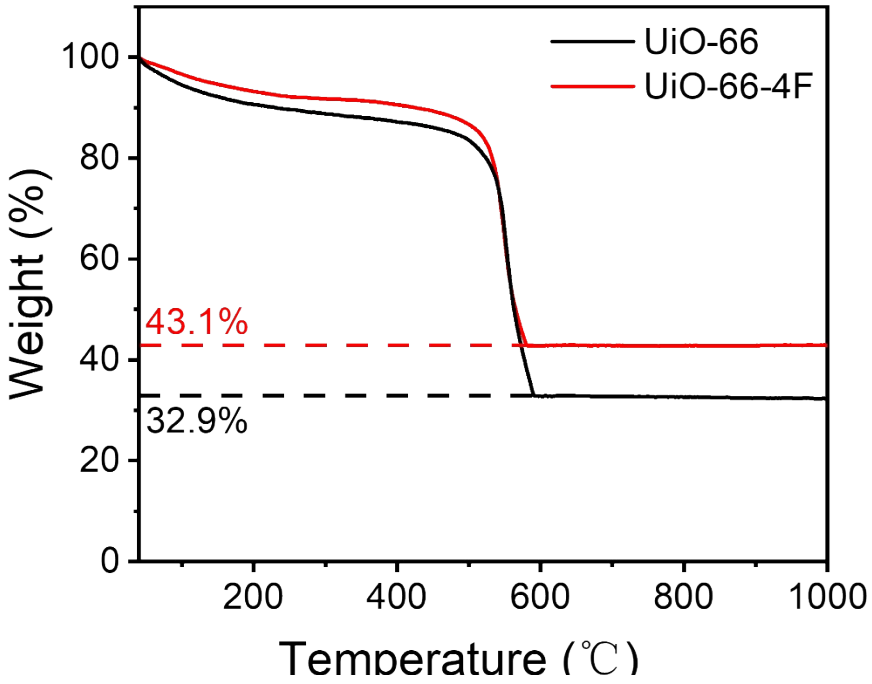

Fig. S3 TGA curves of UiO-66-4F and UiO-66 from 40 ºC to 1000 ºC.

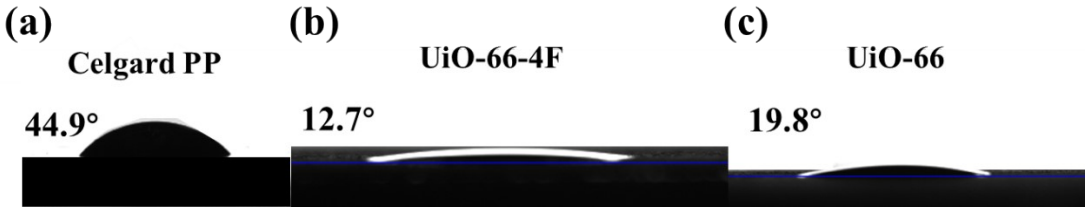

Fig. S4 Contact angle measurements of different separators with electrolytes.

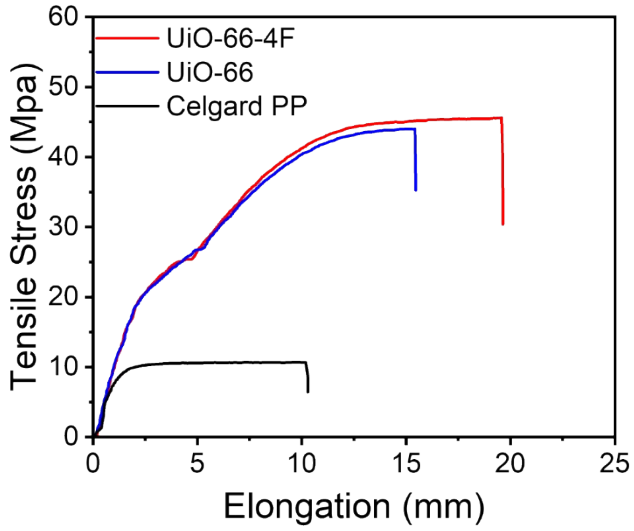

Fig. S5 Tensile-deformation curves of different separators.

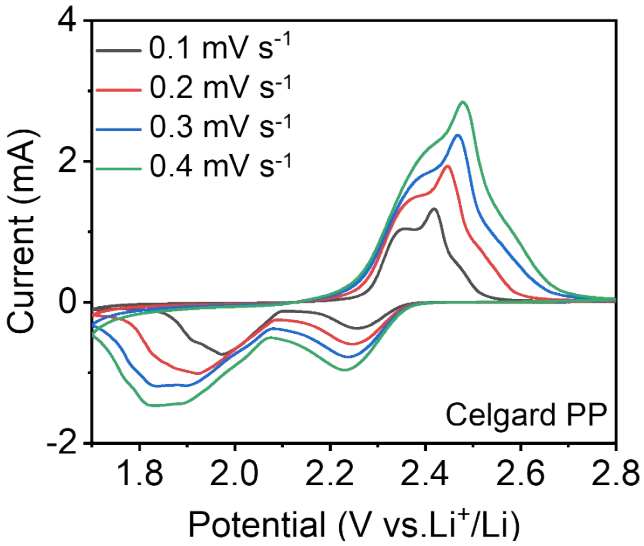

Fig. S6 CV curves of Li-S batteries with Celgard separator at scan rates of 0.1, 0.2, 0.3, 0.4 mV s^{-1}.

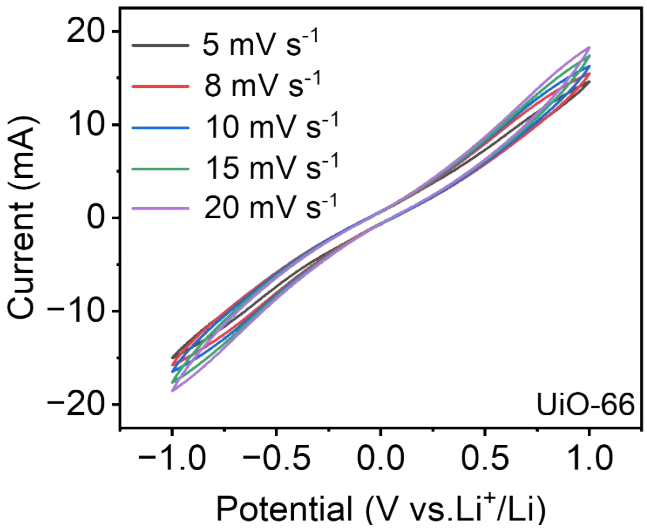

Fig. S7 CV curves of UiO-66 modified separator symmetric cells at different scan. rates.

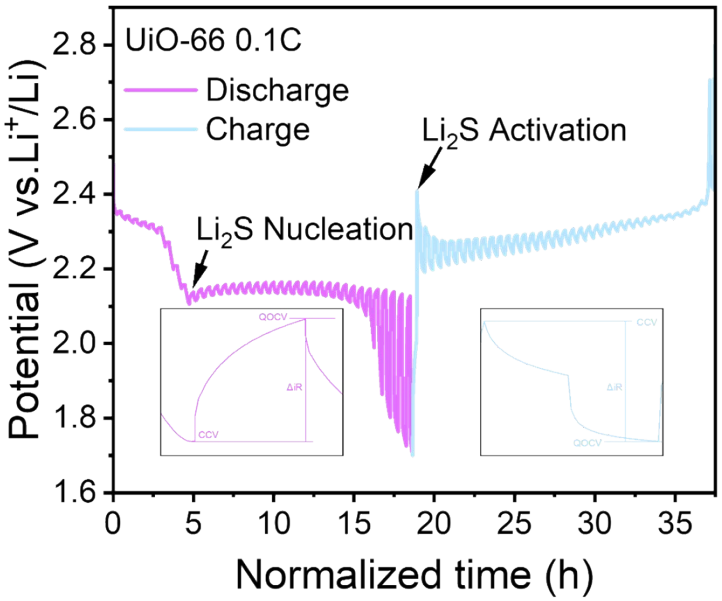

Fig. S8 GITT voltage curves of UiO-66 modified separator batteries at 0.1 C.

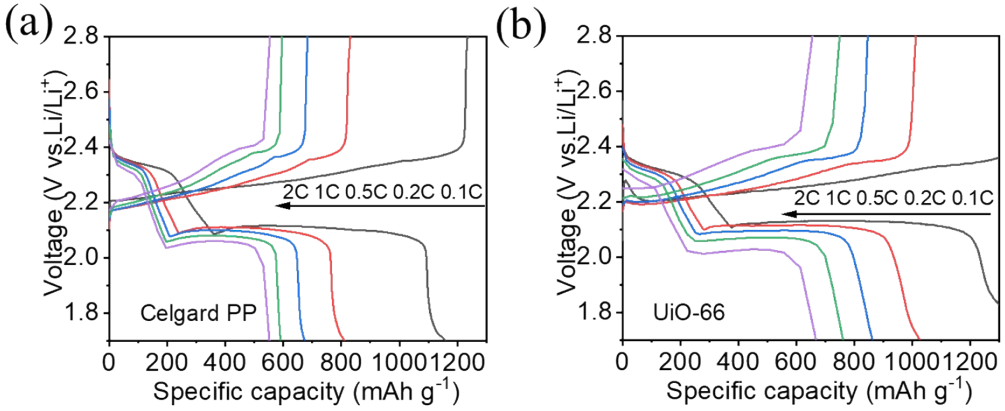

Fig. S9 GCD curves of Celgard PP separator and UiO-66 modified separators batteries at different rates.

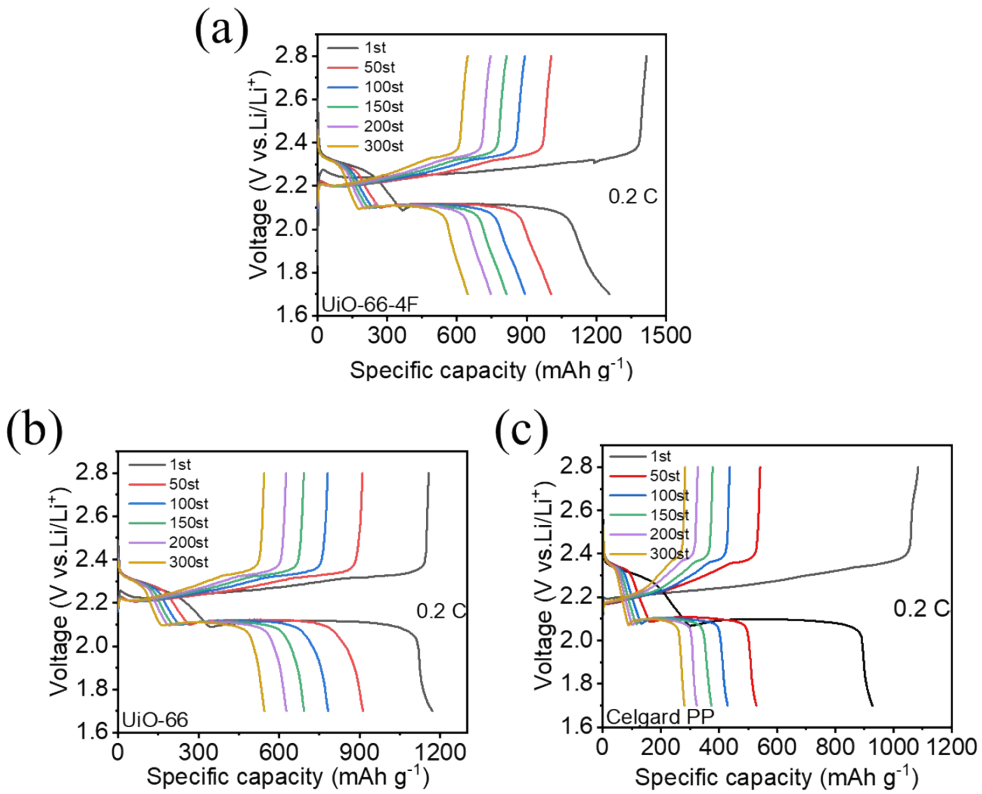

Fig. S10 Charge-discharge curves of different separator batteries at different cycles at 0.2 C.

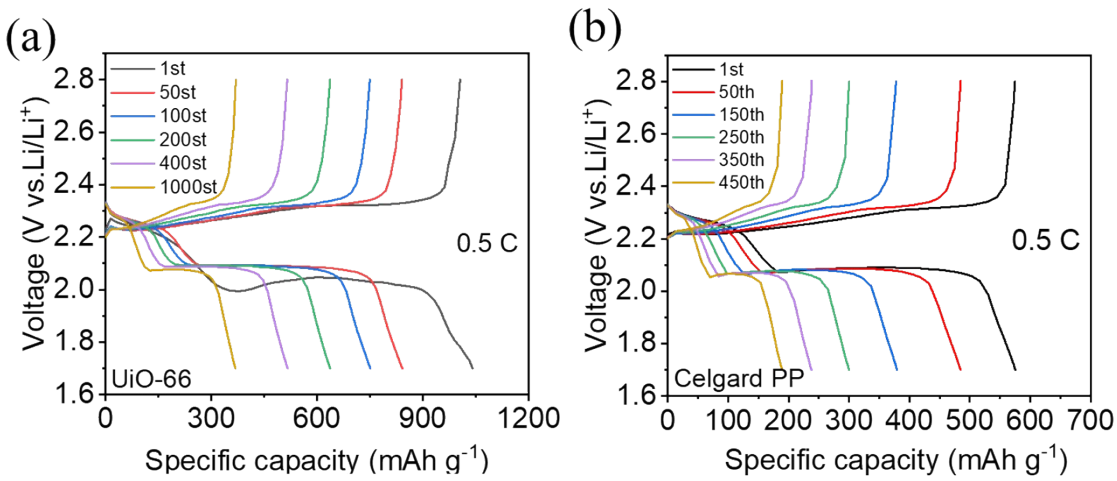

Fig. S11 Charge-discharge curves of different separator batteries at different cycles at 0.5 C.

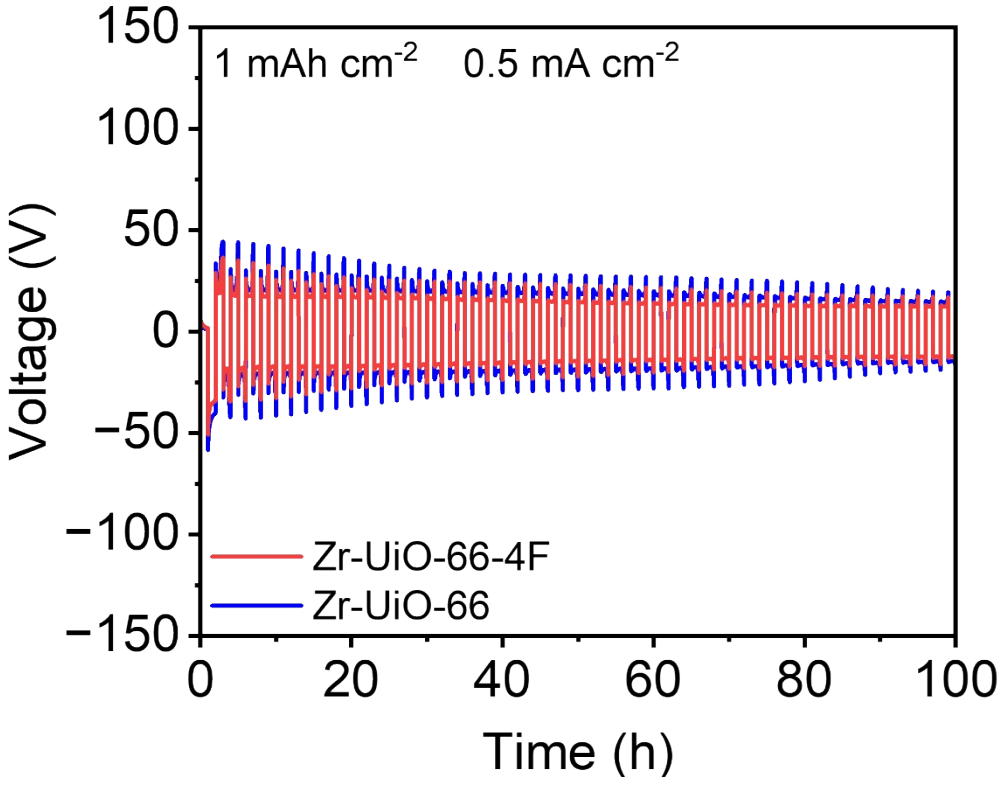

Fig. S12 Voltage profiles of UiO-66-4F and UiO-66 modified separators Li//Li symmetric batteries with a capacity of 1 mAh cm^{-2} at 0.5 mA cm^{-2}.

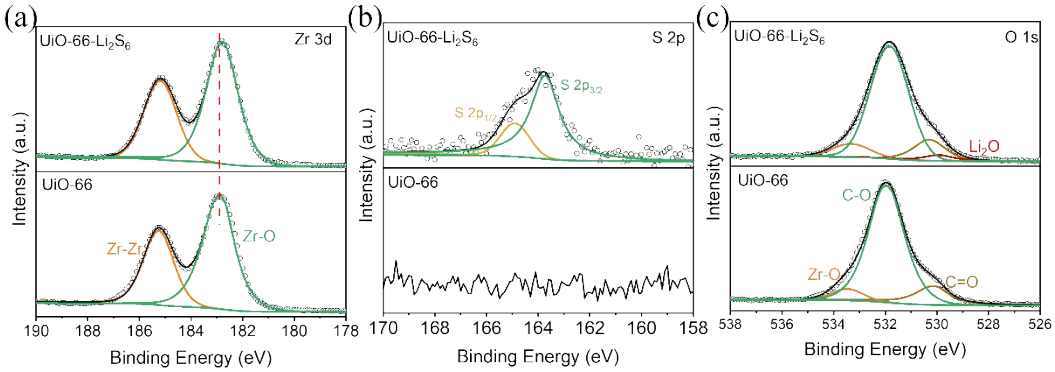

Fig. S13 High resolution XPS spectra of (a) Zr 3d, (b) S 2p, (c) O 1s, and (d) F 1s before and after cycling of UiO-66 modified separator battery at 0.5 C.

Table S1. The atomic composition of UiO-66 and UiO-66-4F.

	C (%)	N (%)	O (%)	F (%)	Zr (%)
UiO-66-4F	64.64	0.54	21.88	10.88	2.06
UiO-66	61.68	0.37	32.10	0	5.84

1. Computational Methods

All density functional theory (DFT) calculations were performed to investigate the interactions between the MOF structures and lithium polysulfides. The computational model, comprising two Zr-oxo nodes connected by one bdc^{2-} linker, was extracted from the crystalline structure of UiO-66 (CCDC: 889529). The unit cell of UiO-66-4F was constructed by modifying the pristine UiO-66 model, followed by full geometric optimization using DFT. For the Brillouin zone integration, gamma-centered meshes with a 2×2×1 k-point grid were employed in reciprocal space.